

Right inferior frontal cortex and preSMA in response inhibition: An investigation based on PTC model[☆]

Lili Wu ^{a,b}, Mengjie Jiang ^{a,b}, Min Zhao ^c, Xin Hu ^c, Jing Wang ^c, Kaihua Zhang ^d, Ke Jia ^{e,f,g}, Fuxin Ren ^{c,*}, Fei Gao ^{c,*}

^a Key Laboratory of Mental Health, Institute of Psychology, Chinese Academy of Sciences, Beijing, China

^b Department of Psychology, University of Chinese Academy of Sciences, Beijing, China

^c Department of Radiology, Shandong Provincial Hospital Affiliated to Shandong First Medical University, Jinan, China

^d School of Psychology, Shandong Normal University, Jinan, China

^e Department of Neurobiology, Affiliated Mental Health Center & Hangzhou Seventh People's Hospital, Zhejiang University School of Medicine, Hangzhou, China

^f Liangzhu Laboratory, MOE Frontier Science Center for Brain Science and Brain-machine Integration, State Key Laboratory of Brain-machine Intelligence, Zhejiang University, Hangzhou, China

^g NHC and CAMS Key Laboratory of Medical Neurobiology, Zhejiang University, Hangzhou, China

ARTICLE INFO

Keywords:

Response inhibition
A pause-then-cancel (PTC) model
Presupplementary motor area (preSMA)
Right inferior frontal cortex (rIFC)
Functional magnetic resonance imaging (fMRI)

ABSTRACT

Response inhibition is an essential component of cognitive function. A large body of literature has used neuroimaging data to uncover the neural architecture that regulates inhibitory control in general and movement cancellation. The presupplementary motor area (preSMA) and the right inferior frontal cortex (rIFC) are the key nodes in the inhibitory control network. However, how these two regions contribute to response inhibition remains controversial. Based on the Pause-then-Cancel Model (PTC), this study employed functional magnetic resonance imaging (fMRI) to investigate the functional specificity of two regions in the stopping process. The Go/No-Go task (GNGT) and the Stop Signal Task (SST) were administered to the same group of participants. We used the GNGT to dissociate the pause process and both the GNGT and the SST to investigate the inhibition mechanism. Imaging data revealed that response inhibition produced by both tasks activated the preSMA and rIFC. Furthermore, an across-participants analysis showed that increased activation in the rIFC was associated with a delay in the go response in the GNGT. In contrast, increased activation in the preSMA was associated with good inhibition efficiency via the striatum in both GNGT and SST. These behavioral and imaging findings support the PTC model of the role of rIFC and preSMA, that the former is involved in a pause process to delay motor responses, whereas the preSMA is involved in the stopping of motor responses.

1. Introduction

Response inhibition is critical for adaptation and navigation in dynamic environments. It refers to the ability to inhibit distractors or inappropriate potential actions to facilitate goal-directed behaviors (Verbruggen and Logan, 2008). Investigating the neural underpinnings of response inhibition will enhance our understanding of the adaptiveness of human beings. A large body of neuroimaging studies provides overlapping evidence of brain activations during response inhibition, comprising the presupplementary motor area (preSMA), the right

inferior frontal cortex (rIFC), and the basal ganglia (Craud and Boulinguez, 2013; Guo et al., 2018; Hung et al., 2018; Isherwood et al., 2021; Simmonds et al., 2008; Swick et al., 2011). The basal ganglia were thought to play a central role in suppressing unwanted movements or thoughts at the subcortical level (Ballanger et al., 2009; Wessel and Aron, 2017). However, the functional specificity of the two cortical regions—the rIFC and preSMA—remains controversial.

Some studies have identified the rIFC as critical in mediating stopping. The rIFC recruitment correlated with the efficiency of response inhibition (Aron et al., 2007; Cai et al., 2014; Xu et al., 2016).

[☆] Fund: This work was supported by the National Natural Science Foundation of China (No. 81601479), Taishan Scholars Project of Shandong Province (No. stsp20240525), Shandong Provincial Natural Science Foundation of China (Nos. ZR2021MH030, ZR2021MH355), and Postdoctoral Innovation Projects of Shandong Province (No. SDCX-ZG-202400047).

* Corresponding author.

E-mail addresses: rxf001@163.com (F. Ren), feigao@email.sdu.edu.cn (F. Gao).

Furthermore, from a temporal perspective, rIFC was found to initiate response inhibition (Schaum et al., 2021). Another study found that rIFC activation was exclusively associated with response inhibition after dissociating inhibitory and non-inhibitory action updating by different tasks (Maizley et al., 2020). However, the results of this study also revealed the influence of preSMA on downstream activation at the subcortical level during stopping, suggesting that it has a critical role in inhibitory control. On the contrary, some studies unveiled that the preSMA is the core region in implementing the stopping, whereas the rIFC is responsible for other forms of control. For instance, the rIFC exhibited enhanced recruitment during more difficult stopping due to an increased working memory load or high time pressure (Hughes et al., 2013; Simmonds et al., 2008). Other studies found that rIFC recruitment is associated with post-stop monitoring (Cao and Cannon, 2021), or attentional reorientation triggered by unexpected events (Sebastian et al., 2021).

The pause-then-cancel (PTC) model, which was first proposed by Schmidt and Berke (2017) based on research in rodents and later extended to humans by Diesburg and Wessel (2021), helps to reconcile the two opposing views regarding the functional specificity of the rIFC and preSMA in response inhibition. This model divides unitary stopping into two successive subprocesses: pause and cancel. The pause process refers to the delay in movement execution triggered by increasing the movement threshold. This is a universal orienting response to infrequent or salient stimuli. The pause process interferes with the go process and biases the stop process. In contrast, the cancel process is theorized to complete the cancellation of a movement or stop the go process. According to the PTC model, the rIFC triggers a pause, whereas the preSMA initiates the cancel process by removing the ongoing prokinetic drive via the striatum.

The EEG technique has high temporal resolution and provides temporal information about the processes that support response inhibition. A late ERP component, a frontocentral P3, is the most common ERP index of successful response inhibition (Schevrelles et al., 2015; Wessel and Aron, 2015). Recent work has evaluated the pause-then-cancel model using the EEG technique. Using a selective stop task, Wadsley et al. (2023) found that the non-signaled hand response was delayed in the partial ignore and partial stop trials compared to the go trials, suggesting a non-selective (global) pause during attention capture. At the neural level, increased frontocentral beta burst modulation (within a 150–250 ms post-stimulus time window) was observed in the partial ignore and partial stop trials compared to the go trials, reflecting the pause process. In another study, Weber et al. (2023) used the electromyogram (EMG) technique and observed reduced muscle activity in trials with ignore cues compared to trials without ignore cues (i.e., infrequent stimuli). Such a decrease in EMG activity could reflect the occurrence of a pause response to ignore cues. Furthermore, Tatz et al. (2021) combined corticospinal excitability (CSE), EMG, and whole-scalp EEG measurements to investigate the early latency signatures of motor inhibition and the neurophysiological signatures specific to action-stopping. They found an early inhibitory process about 150 ms after the stop signal, indicated by corticospinal excitability reduction and EMG suppression. This process was common to all salient events, including valid and invalid stop signals. In contrast, the unique stop process (or the cancel process) occurs later and is indexed by a fronto-centrally distributed P3. Their findings support the PTC model from a temporal perspective.

Although Tatz et al. (2021) provided temporal evidence for the two successive subprocesses indexed by different neural signatures, a direct examination of the associations between the rIFC and preSMA recruitment and motor inhibition based on the PTC model is warranted. For this purpose, we used the GNGT and SST to investigate the functional specificity of the rIFC and preSMA. The GNGT was used to isolate the pause process by including the frequent-go, infrequent-go, and no-go trials. Based on the pause-then-cancel model, a pause process should be elicited in response to infrequent-go but not frequent-go stimuli.

Previous studies have shown that global response inhibition is recruited for salient stimuli, regardless of whether the stimulus signals a need to stop (Dutra et al., 2018; Sebastian et al., 2021). Furthermore, compared to frequent-go stimuli, infrequent-go stimuli evoked a longer reaction time (Chikazoe, Jimura, Asari, et al., 2009; Satoshi et al., 2012), and greater activation in the inferior frontal area (Chikazoe, Jimura, Asari, et al., 2009). Therefore, the inclusion of infrequent-go trials provides a measure of the pause cost by comparing responses between infrequent-and frequent-go trials. Specifically, we examined the associations between rIFC recruitment and the behavioral indices of pauses. To study the cancel process, we examined the association between preSMA recruitment and the behavioral indices of inhibition. In line with the PTC model, we hypothesized that the pause process recruits the rIFC, whereas stopping results in the recruitment of the preSMA. Furthermore, although the PTC model was proposed based on SST, it may be generalized to other action inhibition contexts (Diesburg and Wessel, 2021). Therefore, we further investigate the cross-task generality of the PTC by examining whether neural recruitment during the SST determines the inhibition produced by the GNGT.

2. Method

2.1. Participants

Fifty-six right-handed participants (34 females) were recruited from Shandong First Medical University. All participants were healthy native Mandarin speakers of Chinese Han ethnicity with normal or corrected-to-normal vision. Before the experiment, participants provided informed consent. The Institutional Review Board of Shandong First Medical University approved this study.

Data from three participants (all female) were excluded from analysis due to their low accuracy (<70%) on the go trials when performing either task. A further 14 participants (8 female) with excessive head movements (greater than 2 mm or 2°) in either or both tasks were therefore excluded from all data analyses.¹ After removing these 17 participants, the final study sample was 39 (23 female; age range 22–35 years; $M_{age} = 28.49$ years; and $SD = 3.55$).

2.2. Experimental design

Go/No-go task. The GNGT consisted of two blocks, each consisting of 80 trials. Three types of stimuli were presented: the frequent-go stimuli (the letter 'M'), the infrequent-go stimuli (the letter 'N'), and the no-go stimuli (the letter 'W'). In each block, 40 trials (50%) presented the frequent-go stimuli, 20 trials (25%) presented the infrequent-go stimuli, and 20 trials (25%) presented the no-go stimuli.

These three types of trials were presented randomly, with the setting that no more than three go stimuli (frequent-go and infrequent-go) were presented within each consecutive 6-s period. In each trial, the stimuli were presented in the center of the screen for an 800 ms duration. The participants were required to press a button with their right index finger quickly and accurately when the stimuli (frequent-go and infrequent-go) signified a 'go' response and to withhold their motor response when the stimuli (no-go) signified a 'no-go' response. The stimuli disappeared after the participants pressed the buttons, and a fixation cross was presented until the presentation of the next trial. The stimulus onset asynchrony (SOA) between stimuli was pseudo-randomly set at 2000 or 4000

¹ Participants first performed the GNGT and then the SST. When performing the GNGT, eight participants had head motions larger than 2 mm or 2 degrees in either of the two blocks. When performing the SST, 12 participants had head motions larger than 2 mm and 2 degrees in either of the two blocks. There was some overlap between these participants. Therefore, 14 participants were excluded. The number of excluded participants was higher for the SST than for the GNGT, possibly due to fatigue.

ms.

Stop signal task. The SST consisted of two blocks, each consisting of 120 trials. Each block had frequent (75%, identical to the ratio of go trials in the GNGT) go trials to set up a pre-potent response tendency, and less frequent (25%, identical to the ratio of no-go trials in the GNGT) stop trials for participants to withhold their response. In total, the SST contained 180 go trials and 60 stop trials.

In the go trial, the go stimuli (right or left arrow) were presented in the center of the screen for 800 ms. The participants responded to the arrow stimulus by pressing the right or left buttons. The participants were instructed to respond quickly and accurately. The go stimuli disappeared when the button was pressed, and a fixation was presented until the presentation of the next stimuli. In a stop trial, after the presentation of go stimuli, an additional "X" of the stop signal appeared. The participants were instructed to withhold their motor responses after detecting the stop signal. The stop signal vanished if the participants pressed the buttons or after 800 ms had elapsed, whichever occurred first. The task used a staircase design for the stop signal delay (SSD) to adapt to the performance of the participant and narrow the 50% success rate for inhibition. The SSD started at 200 ms and varied from one stop trial to the next according to the staircase procedure. If the participant succeeded in withholding the response, the SSD increased by 50 ms. Conversely, if they failed, the SSD decreased by 50 ms. After the disappearance of the Stop signal, a fixation was presented until the presentation of the next stimuli. The stimulus onset asynchrony (SOA) between stimuli was randomly set to 2000 or 4000 ms.

2.3. fMRI procedure

The MRI data acquisitions were conducted using an 8-channel phased-array head coil on a 3.0 MRI scanner (Philips, Achieva TX, Netherlands). Earplugs and soft foam padding were used to minimize head movement and ambient noise. The structural data acquisition was performed using a T1-weighted 3D turbo field echo sequence with repetition time (TR) of 8.1 ms, echo time (TE) of 3.7 ms, field of view (FOV) of 240 mm × 240 mm, voxel size of 1 mm × 1 mm × 1 mm, and slice thickness of 1 mm.

Functional data were obtained via an echo planar imaging (EPI) sequence based on blood oxygenation level-dependent (BOLD) with TR of 2000 ms, TE of 30 ms, flip angle of 90°, a field of view of 224 mm × 224 mm, voxel size of 3.5 mm × 3.5 mm × 3.5 mm, slice thickness of 3.5 mm and image matrix of 64 × 64.

2.4. Behavioral data analysis

For GNGT, the reaction time and accuracy for infrequent-go and frequent-go trials were calculated, respectively. An index measuring the delay in the go process due to the pause mechanism was defined as the difference between the reaction time for infrequent-go trials and frequent-go trials. Furthermore, a prior study defined that participants who make faster go responses in infrequent-go trials and a higher percentage of correct stops in no-go trials ought to be regarded as more efficient performers (Satoshi et al., 2012). Therefore, they defined an index describing the individual difference in inhibition efficiency, reflecting the good performance on both no-go and infrequent-go trials. To calculate this efficiency index, both the percentage of correct performance in no-go trials and the reaction time in the infrequent-go trials were standardized, and then subtracted the standardized reaction time from the standardized percentage of correct performance. Here, a larger efficiency index represents a higher percentage of correct performance in no-go trials and a shorter reaction time in go trials.

For SST, the stop-signal reaction time (SSRT) was computed as the main index of response inhibition efficiency. It was estimated for each participant using the integration method (Logan and Cowan, 1984; Satoshi, et al., 2012).

2.5. fMRI data analysis

Image preprocessing and statistical analysis were performed using SPM12 software (<https://www.fil.ion.ucl.ac.uk/spm/software/spm12/>). Preprocessing included slice-time correction, head motion realignment, coregistration with individual structural images, segmentation, normalization to a Montreal Neurological Institute (MNI) template and resampling to create 3.5-mm isotropic voxels, and spatially smoothing by using a Gaussian filter with 8-mm full-width half maximum.

At the individual level, four separate regressors were created and time-locked to the onset of stimuli presentation (successful frequent-go, successful infrequent-go, successful no-go, and failures in both no-go and go trials) within the GNGT task. In the SST task, three separate regressors were created and time-locked to the onset of stimulus presentation (successful go, successful stop, and failed stop). Additionally, six realignment parameters were included to account for head movement-related variability. A high-pass filter with a cut-off frequency of 1/128 Hz was used to correct for low-frequency components and serial correlations using an autoregressive AR (1) model.

2.6. Contrast analysis

To evaluate the neural basis involved in response inhibition, the contrast of successful no-go vs. successful frequent-go in the GNGT, and the contrast of successful-stop vs. successful go in the SST were generated. To investigate the core response inhibition system, we further examined the common regions of brain activation in response inhibition between the GNGT and the SST. We used the activated region related to response inhibition during the SST as a mask (FWE correction, $p < .05$, cluster >5). Subsequently, we applied it to generate response inhibition-related activation in the GNGT with a threshold of $p < .05$ (FWE corrected) and more than 5 voxels.

To evaluate the neural basis involved in the pause/orienting process, the contrast of successful infrequent-go vs. successful frequent-go in the GNGT was generated. According to the PTC model, the failed stop trials also recruited the pause/orienting process (Diesburg and Wessel, 2021). Therefore, the contrast of failed-stop vs. successful-go in the SST was generated. For the whole-brain exploratory search, the threshold was set at $p < .05$ (FWE corrected) with more than 5 voxels.

2.7. Across-participants correlation analysis

To examine rIFC recruitment in the pause process, and the presMA recruitment in the cancel process, we conducted a correlation analysis between brain recruitment and the behavioral index indicating pause and inhibition. According to the PTC model, the cancel process is initiated by the preSMA by removing the ongoing prokinetic drive via the striatum. Thus we examined the activation in the striatum when investigating the cancel process.

To conduct the correlation analysis, we defined three ROIs in the rIFC (MNI: $x = 50, y = 16, z = 18$; radius = 10 mm), preSMA (MNI: $x = 4, y = 18$, and $z = 46$; radius = 10 mm), and striatum (MNI: $x = 14, y = 8, z = 6$; radius = 10 mm) based on a previous meta-analysis of response inhibition (Cai et al., 2014) (Supplementary material, Fig. 1S). Previous literature showed that GNGT and SST recruit different regions within the medial frontal cortex (e.g., Mcnab et al., 2008; Zheng et al., 2008; Dambacher et al., 2014; Guo et al., 2018). Thus, we also defined an additional ROI in preSMA (MNI: $x = -8, y = 20, z = 44$; radius = 10 mm, based on Rae et al., 2015) for examining the correlation between preSMA and inhibition index in GNGT. The activation (beta value) within these four ROIs was extracted by Marsbar (v0.45; <http://marsbar.sourceforge.net>) (Brett et al., 2002).

2.8. Brain activation-behavior relationship

Pause/orienting mechanism. We first tested whether the rIFC was

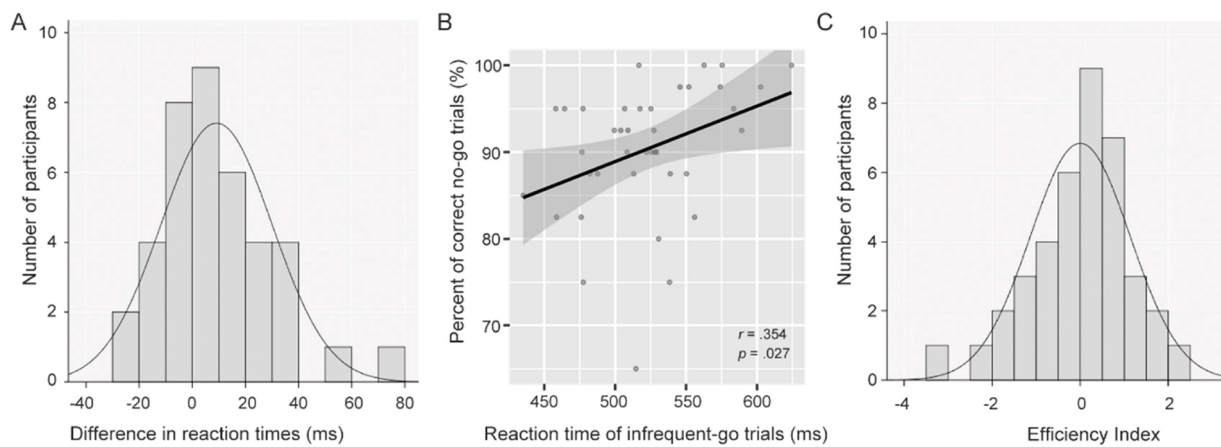


Fig. 1. A, The distribution of the efficiency index. B, The distribution of the reaction time in the successful infrequent-go trials and the percentage accuracy in the no-go trials. One dot represents one participant. C, The distribution of the efficiency index.

involved in the pause process. To do this, an index of delay in go response due to the pause mechanism for each participant was calculated by subtracting the mean reaction time in the successful frequent-go trials from the mean reaction time in the successful infrequent-go trials in GNGT. The pause-related brain activity for each participant was obtained by subtracting the extracted brain activation in the successful frequent-go trials from the extracted brain activation in the successful infrequent-go trials.

Cancel mechanism. To test that the preSMA is involved in the implementation of stopping, we first examined the correlation between the extracted activations in preSMA and inhibition efficiency. Specifically, we examined the association between the extracted activations in preSMA in successful no-go trials and the efficiency index for inhibition in GNGT, and the correlation between the extracted activations in pre-SMA in successful-stop trials and SSRT in SST. Considering that preSMA implement stopping by the striatum, we also examined the correlation between the extracted activations in the striatum and inhibition efficiency in GNGT and SST, respectively. Next, we conducted mediating analyses to determine whether the preSMA implemented the stop via the striatum. The mediation model was tested using the PROCESS macro for the SPSS (Model 4) computational tool (Hayes, 2017). The indirect effect was estimated using bootstrapping procedures (bootstrap sample = 10,000).

Furthermore, to test the cross-task generality of the PTC, we examined whether or not neural recruitment of preSMA and striatum during SST determines the inhibition in GNGT.

3. Results

3.1. Behavioral results

In the GNGT, the mean percentage of correct performance was 98.11% ($SD = 4.91\%$), 98.53% ($SD = 5.64\%$), and 90.32% ($SD = 7.66\%$) in the frequent-go, infrequent-go, and no-go trials, respectively. The difference in the percentage of correct performance between the successful frequent-go and the successful infrequent-go trials was not significant ($t(38) = -1.32, p = .20, d = -0.21, 95\%CI: -0.527, 0.108$). Mean reaction times were 513.13 ms ($SD = 42.99$) and 522.14 ms ($SD = 42.34$) in the successful frequent-go and the successful infrequent-go trials, respectively. The difference in mean reaction times between frequent-go and infrequent-go trials was significant ($t(38) = -2.65, p = .01, d = -0.42, 95\%CI: -0.749, -0.093$). A balanced distribution of the delay in the go response was obtained by subtracting frequent-go trials' reaction time from infrequent-go trials' reaction time (Fig. 1A). The difference in reaction times was not significantly different from a normal one as tested by the Shapiro-Wilk test ($W = 0.945, p = 0.06$).

The reaction time to the infrequent-go stimulus and the percentage of successful stop to the no-go stimulus were significantly correlated ($r(37) = 0.354, p = .027, 95\%CI: 0.043, 0.602$, Fig. 1B). As a prior study defined (Satoh et al., 2012), an efficient index that reflects a fast response in infrequent-go trials and a high percentage of correct stops in no-go trials was calculated. A balanced distribution of this efficiency index was obtained (Fig. 1C). This index was not significantly different from a normal one as tested by the Shapiro-Wilk test ($W = 0.973, p = 0.461$).

In the SST, the mean percentage of correct performance was 91.62% ($SD = 6.92\%$) and 54.71% ($SD = 4.11\%$) in the go and stop trials, respectively. The mean reaction time in the successful go trials was 573.47 ms ($SD = 79.76$). The failed stop response (commission errors) RT was 532.13 ms ($SD = 82.53$). Reaction times in failed stop trials were faster than go reaction times for each participant and at the group level ($t(38) = 14.02, p < .001, d = 2.25$). This suggests that the assumptions of the race model are met, which requires that the reaction times in the failed stop trials fall on the left side of the go reaction times distribution. The mean SSD was 309.88 ms ($SD = 92.94$), and the mean SSRT was 238.38 ms ($SD = 43.64$). The correlation between the efficiency index in GNGT and SSRT was significant ($r(37) = -.365, p = .022, 95\%CI: -0.610, -0.056$).

3.2. fMRI results

3.2.1. Contrast results

The brain activation associated with response inhibition was calculated based on the contrast of “successful no-go versus successful frequent-go” in the GNGT (Table 1), and the contrast of “successful stop versus successful go” in the SST (Table 2). Prominent activations were found in multiple regions, including the rIFC-preSMA circuit (Fig. 2).

The overlap in brain areas supporting response inhibition mainly included the bilateral inferior frontal area/insula, preSMA, and middle frontal gyrus in GNGT and SST (Table 3, Fig. 3).

To examine whether the rIFC was involved in the pause process, we examined the contrast between successful infrequent-go and successful frequent-go trials in GNGT, and the contrast between the failed stop and successful go trials in SST. The former contrast generated no significant regions while the latter generated significant regions in rIFC (Fig. 4, Table 4).

3.3. Brain-behavior relationships

We first examined the association between rIFC recruitment and the pause process by performing correlational analyses. Specifically, we examined the correlation between the delay in go trials and the

Table 1

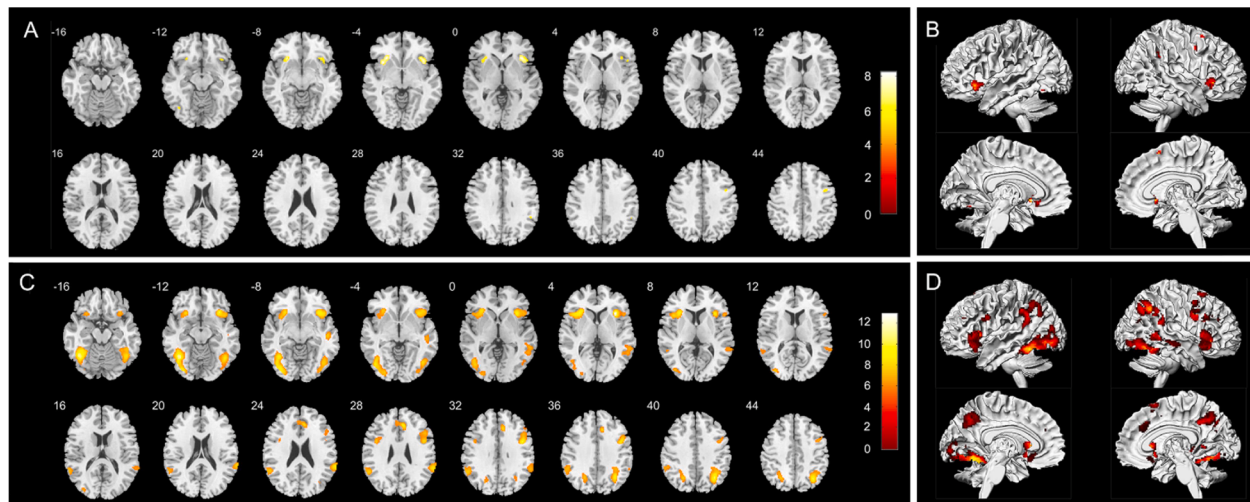
Brain areas showing signal increase in the contrast of “successful no-go versus successful frequent-go” in GNGT.

Anatomical Regions	BA	Hemisphere	Peak MNI Coordinates			cluster size (voxels)	t-value
			x	y	z		
Insula/inferior frontal gyrus	47	L	-36	16	-4	163	8.20
Insula/inferior frontal gyrus	47	R	36	20	-2	216	8.18
preSMA	6	R	20	12	60	13	6.96
Middle Frontal Gyrus	6	R	40	4	44	32	6.32
Inferior occipital gyrus	19	L	-44	-66	-12	5	5.79
Supramarginal Gyrus	40	R	48	-44	32	8	5.77

Note: FWE $p < .05$. BA: Brodmann Area.**Table 2**

Brain areas showing signal increase in the contrast of “successful stop versus successful go” in SST.

Anatomical Regions	BA	Hemisphere	Peak MNI Coordinates			cluster size (voxels)	t-value
			x	y	z		
Inferior frontal gyrus	47	R	30	20	4	860	12.85
Fusiform gyrus	37	L	-42	-58	-14	1607	11.83
Insula/Inferior frontal gyrus	47	L	-32	22	6	768	10.21
Angular gyrus	7	R	32	-60	38	672	10.20
Middle frontal gyrus	6	R	42	4	32	592	10.02
Anterior cingulate	32	R	6	34	26	246	9.59
Supramarginal gyrus	40	R	62	-42	24	783	8.87
Fusiform	37	R	42	-62	-12	818	8.66
preSMA	6	R	14	16	62	75	8.04
Supramarginal gyrus	40	L	-58	-52	30	445	7.75
Inferior parietal gyrus	7	L	-26	-62	38	337	7.65
Inferior frontal gyrus	9	L	-44	4	28	95	7.46
Supplementary motor area	8	R	4	18	54	9	5.85
Middle temporal gyrus	39	R	36	-72	22	7	5.68

Note: FWE $p < .05$. BA: Brodmann Area.**Fig. 2.** Brain regions involved in response inhibition in GNGT (A and B) and SST (C and D).**Table 3**

Common brain areas involved in response inhibition in both GNGT and SST.

Anatomical Regions	BA	Hemisphere	Peak MNI Coordinates			cluster size (voxels)	t-value
			x	y	z		
Insula/inferior frontal gyrus	47	L	-36	16	-4	154	8.20
Insula/inferior frontal gyrus	47	R	36	20	-2	214	8.18
preSMA	6	R	20	12	60	5	6.96
Middle frontal gyrus	6	R	40	4	44	23	6.32
Inferior occipital gyrus	19	L	-44	-66	-12	5	5.79

Note: FWE $p < .05$. BA: Brodmann Area.

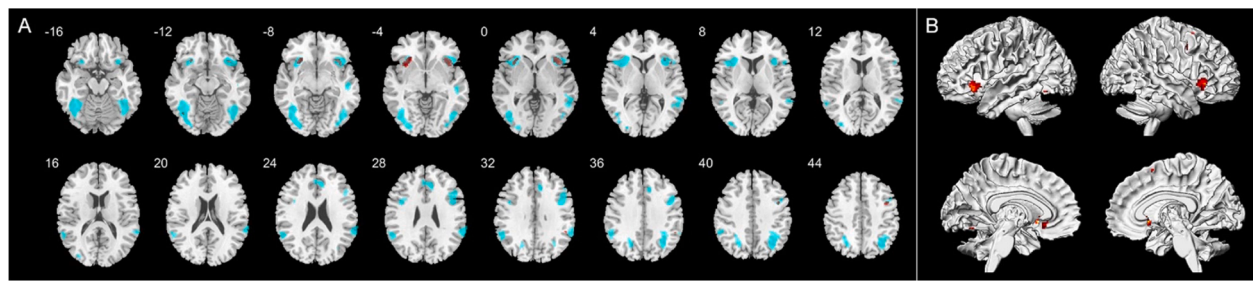


Fig. 3. Regions that were involved in response inhibition in GNGT (red) or SST (blue)(A) and rendered images for the overlaps(B).

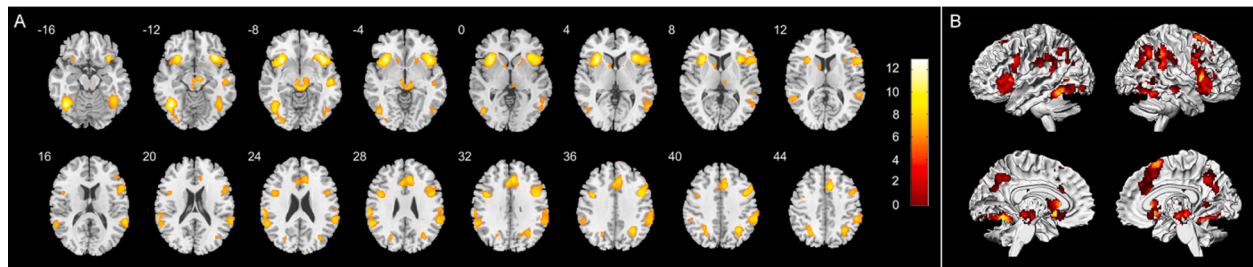


Fig. 4. Brain activations during failed stop trials than during successful go trials (A: image of slices; B: rendered images for activations).

Table 4
Brain areas showing signal increase in the contrast of “failed stop versus successful go” in SST.

<i>Anatomical Regions</i>	<i>BA</i>	<i>Hemisphere</i>	<i>Peak MNI Coordinates</i>			<i>cluster size (voxels)</i>	<i>t-value</i>
			<i>x</i>	<i>y</i>	<i>z</i>		
Fusiform	37	L	-44	-58	-12	1078	12.45
Insula/Inferior frontal gyrus	47	R	34	22	-10	2565	12.23
Insula/Inferior frontal gyrus	13	L	-32	16	-8	1158	11.96
Sub-gyrals	7	R	28	-58	38	556	9.76
Brainstem	-	L	-4	-30	-8	450	9.74
Superior frontal gyrus	32	R	8	18	46	1649	9.72
Middle temporal gyrus	22	R	50	-22	-8	170	8.89
Precentral gyrus	9	L	-42	4	34	370	8.88
Supramarginal gyrus	40	L	-58	-44	28	717	8.56
Superior temporal gyrus	40	R	60	-44	16	1202	8.47
Fusiform	37	R	40	-50	-14	665	8.20
Superior parietal lobule	7	L	-28	-62	44	300	8.01
Caudate nucleus	-	L	-12	8	10	98	6.73
Thalamus	-	R	6	-20	8	20	6.50
Corpus callosum	-	R	4	-24	26	7	5.78

Note: FWE $p < .05$. BA: Brodmann Area.

increased activation in the rIFC during successful infrequent-go trials compared to successful frequent-go trials. Activation in the rIFC (successful infrequent-go minus successful frequent-go) correlated with the delay in the go response, $r(37) = 0.329$, $p = .041$, 95%CI: 0.015, 0.584 (Fig. 5A).

Next, to test the hypothesis that the preSMA is involved in the cancel process, we correlated the activation in the preSMA during the successful no-go trials with the inhibition efficiency index in the GNGT. Activation in the preSMA during the no-go trial was associated with the inhibition efficiency index, $r(37) = 0.333$, $p = .038$, 95%CI: 0.020, 0.587 (Fig. 5B). In contrast, the correlation between activation in the striatum during the no-go trial and the inhibition efficiency index was positive but not significant, $r(37) = 0.210$, $p = .199$, 95%CI: -0.113, 0.493. For the SST, the correlation between the preSMA activation during successful stop trials and inhibition efficiency indexed by SSRT was not significant, $r(37) = -.019$, $p = .907$, 95%CI: -0.298, 0.333. However, the correlation between the striatum activation during successful stop trials and inhibition efficiency indexed by SSRT was significant, $r(37) = -.320$, $p = .047$, 95%CI: -0.577, -0.005 (Fig. 5C).

In addition, to investigate whether the preSMA activity contributes to the pause and thus may correlate with the go delay, and vice versa for rIFC and inhibition efficiency, we tested the correlation between the preSMA activity and the pause, and the correlation between rIFC activity and inhibition efficiency. The correlation between the preSMA activity during the no-go trials and the pause cost in go trials was not significant ($r(37) = -.086$, $p = .601$, 95%CI: -0.391, 0.236). Similarly, the correlation between rIFC activity (successful infrequent-go minus successful frequent-go) and the inhibition efficiency indices of both GNGT and SST were not significant (for GNGT: $r(37) = -.073$, $p = .659$, 95%CI: -0.380, 0.248; for SST: $r(37) = 0.002$, $p = .988$, 95%CI: -0.313, 0.318).

Furthermore, the mediating analysis showed that activation in the preSMA predicted the activation in the striatum ($\beta = 0.509$, $t = 4.177$, $p < 0.001$), which in turn preceded the SSRT ($\beta = -34.672$, $t = -2.632$, $p = 0.012$). The indirect effect of BOLD activation in the striatum was significant between the activation in preSMA and inhibition efficiency indexed by SSRT (see Fig. 6).

We also examined the mediating effect of striatum activation in no-go trials between the preSMA activation in no-go trials and inhibition

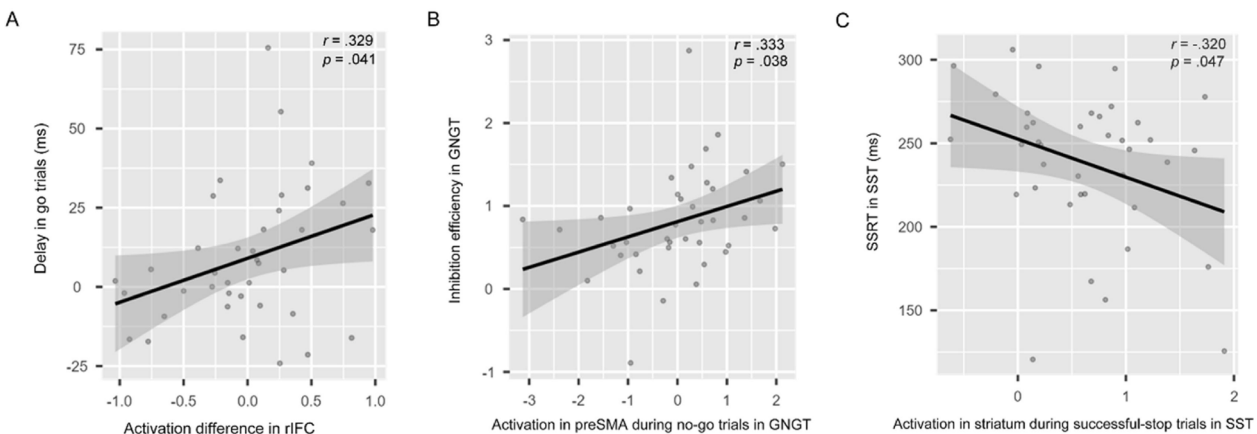


Fig. 5. Correlations between brain activations and behavioral indices in GNGT and SST. A, The distribution of the difference in rIFC activation (successful infrequent-go minus successful frequent-go) and the delay in go response (successful infrequent-go minus successful frequent-go) in GNGT. B, Distribution of the preSMA activation during successful no-go trials and the inhibition efficiency in GNGT. C, Distribution of the striatum activation in successful stop trials and the inhibition efficiency in SST. One dot represents one participant.

efficiency in GNGT. The mediating model was not significant.

Next, we examined whether the activation in preSMA and striatum during successful stop trials would predict the inhibition efficiency in GNGT. The mediating analysis showed that activation in the preSMA predicted the activation in the striatum ($\beta = 0.509$, $t = 4.177$, $p < 0.001$), which in turn preceded the inhibition efficiency in GNGT ($\beta = 0.8614$, $t = 2.491$, $p = 0.018$). The indirect effect of BOLD activation in the striatum on a successful stop trial was significant between the activation in preSMA on a successful stop trial and inhibition efficiency in GNGT (Fig. 7).

4. Discussion

The rIFC and the preSMA have been repeatedly observed to be involved in response inhibition. However, there are controversies regarding their specific role. The PTC model resolves the controversy over the functional specificity of rIFC and preSMA during response inhibition by dividing the unitary inhibition process into two subprocesses - a salience-related pause and a stop-specific cancel process (Diesburg and Wessel, 2021). The current study tested the functional specificity of rIFC and preSMA in response inhibition based on the PTC model. To do this, we specifically examined the association between brain recruitment and the behavioral index of the pause and cancel process, respectively.

The imaging results showed that response inhibition in both GNGT and SST recruited multiple brain regions, including the rIFC, preSMA,

anterior insula, and bilateral parietal area, which is consistent with previous empirical findings (Chikazoe, Jimura, Asari, et al., 2009, 2009; Maizley et al., 2020; Mostofsky et al., 2003; Nakata et al., 2008) as well as previous meta-analysis findings (Cai et al., 2014; Isherwood et al., 2021; Simmonds et al., 2008). Consistent with the PTC model, failed stop trials involved more recruitment in rIFC than go trials, indicating the enhanced pause mechanism. The across-participants analysis revealed that the pause cost (successful infrequent-go versus successful frequent-go) in go response increased as the pause-related activity (successful infrequent-go versus successful frequent-go) in rIFC enhanced, suggesting the involvement of rIFC in the pause process. In contrast, the preSMA activation predicted the inhibition efficiency in both GNGT and SST. Moreover, the implementation of the stopping supported by preSMA and striatum in SST could be generalized to GNGT, indicating the cross-context generalization of the cancel mechanism. Together, the present findings thus provide direct evidence for the PTC model.

According to the PTC model, the pause process recruits a hyperdirect pathway, which raises the threshold for motor execution, thus postponing the go process (Diesburg and Wessel, 2021). In the current study, we used the GNGT to isolate and examine the pause mechanism. The behavioral results showed that the response time to infrequent-go stimuli was longer than the response time to frequent-go stimuli, reflecting a delay in motor execution. This finding is consistent with previous studies (Chikazoe, Jimura, Asari, et al., 2009; Satoshi et al.,

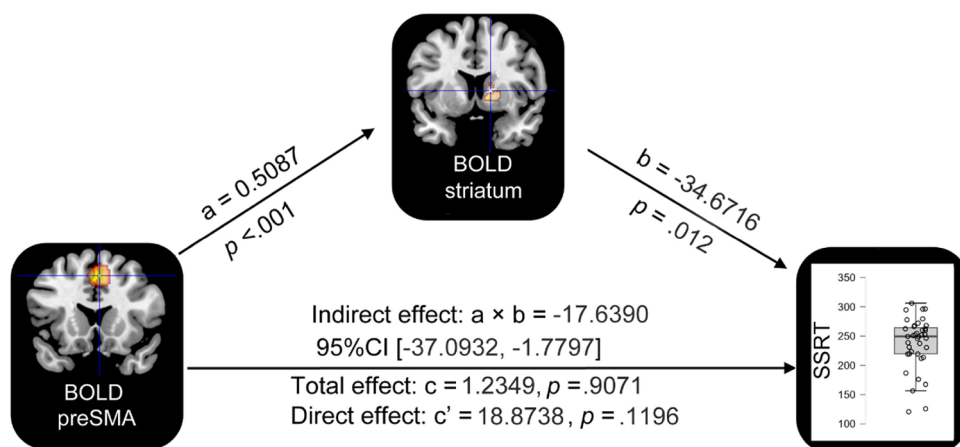


Fig. 6. The relationship between preSMA activation and the inhibition efficiency indexed by SSRT in SST was mediated by activation in the striatum. Crosshairs indicate the central coordinates of the two ROIs, respectively. Unstandardized regression coefficients are shown for each path.

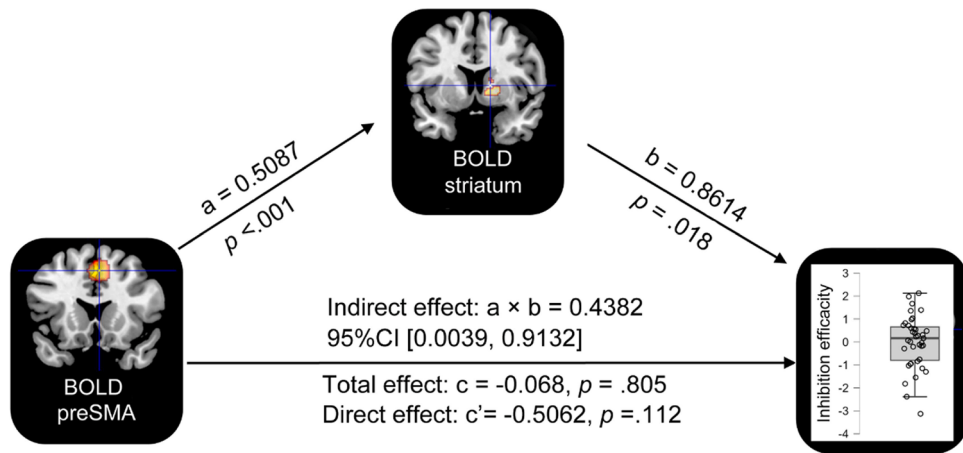


Fig. 7. The relationship between preSMA activation in successful-stop trials and the inhibition efficiency in GNGT was mediated by activation in the striatum on successful-stop trials. Crosshairs indicate the central coordinates of the two ROIs, respectively. Unstandardized regression coefficients are shown for each path.

2012). Across-participants analysis showed that a larger delay in the go response was associated with enhanced activation of the rIFC in infrequent-go trials than in frequent-go trials, providing direct evidence for the salience-detecting pause mechanism. This is consistent with previous findings that delay in motor generation recruits increased activation in the right inferior frontal area (Chikazoe, Jimura, Asari, et al., 2009). These findings are also consistent with a previous study that revealed that increased recruitment of the fronto-basal-ganglia network during the unexpected go condition was associated with a stronger response slowing on unexpected go events compared with regular go events (Sebastian et al., 2021).

Theoretically, there are two main perspectives regarding the role of rIFC. The first conceptual function of rIFC is to initiate the inhibition process (Aron et al., 2014). In contrast, the other view perceives the rIFC as being within the right frontoparietal network, responsible for salience detection and attention direction (Corbetta et al., 2008; Corbetta and Shulman, 2002). This region is recruited during response inhibition, but is also activated in conditions where important cues are detected without a motor response (Hampshire, 2015; Hampshire et al., 2010). The PTC model conceptualizes the rIFC as being involved in the pause process, which can be further regarded as a universal orienting response to salient events, as salient stimuli trigger the pause process (Diesburg and Wessel, 2021). A recent study further supported the view that rIFC primarily detects salient signals (Choo et al., 2022).

Several past psychophysiological studies have revealed that orienting contains three subcomponents: automatic detection of sensory change, an attention switch to the salient or novel event, and voluntary attentional reorienting to the task (Reisenzein et al., 2012). We believe the positive association between rIFC recruitment and delay in go responses may reflect the subcomponent of detecting salient events (i.e., infrequent-go stimuli). Such detection of the sensory change and attention switch to a salient event can cause a delay in motor execution.

The contrast between the successful no-go/stop trials and successful go trials revealed strong activation in the preSMA. When we looked at the common areas involved in response inhibition between the GNGT and SST, the results showed overlapped areas in the rIFC, but little overlap within the preSMA. This is consistent with previous literature, which found that although the preSMA is involved in response inhibition (Dambacher et al., 2014; Isherwood et al., 2021), the specific locations of activated clusters within preSMA differ between GNGT and SST (e.g., Mcnab et al., 2008; Zheng et al., 2008; Dambacher et al., 2014; Guo et al., 2018). Furthermore, SST recruited more activations in preSMA than GNGT. These differences in preSMA involvement likely reflect the differences in cognitive operations between these two tasks (Raud et al., 2020). The SST involves more top-down control than the GNGT (Littman and Takacs, 2017; Raud et al., 2020). Furthermore, Guo et al. (2018)

found that the SST shared more common brain activations with memory inhibition tasks in the frontal area including preSMA, whereas the GNGT shared limited brain regions with the memory inhibition task. Their findings also suggest that the GNGT may be less demanding on working memory than the SST, resulting in less activation in the preSMA.

Furthermore, activation of the preSMA directly predicted the response efficiency in the GNGT and was indirectly associated with the inhibition index in the SST. These findings together suggested that preSMA is involved in the implementation of the stop process. According to the PTC model, the cancel process stops by an indirect pathway via the striatum (Diesburg and Wessel, 2021). Specifically, the preSMA sends signals to the striatum, which in turn removes the direct basal ganglia pathway drive for movement. In support of this view, the mediation model showed that increased activation in the preSMA was associated with increased activation in the striatum, which in turn was associated with a high inhibition efficiency in the SST. The GABAergic output from the striatum modulates the basal ganglia neural activation (Hikosaka, 2007). A previous study showed that high GABA levels in the striatum were associated with better response inhibition (Quetscher et al., 2015). Therefore, to further elucidate the interactions of the preSMA-striatum circuit in inhibition, future studies should include GABAergic signal measurements.

A particular strength of the present study is that we administered the SST and GNGT to the same group of participants, which allowed a direct examination of the cross-task generality of the cancellation mechanism. Previous studies identifying the core response inhibition mechanisms have primarily focused on overlapping evidence in brain activations of separate tasks (e.g., Mostofsky et al., 2003; Zheng et al., 2008; Isherwood et al., 2021). These studies promote knowledge of the neural underpinnings of response inhibition. The present study extends the results of prior studies by examining whether the extent of neural involvement of the preSMA and striatum also contributes to the efficiency of GNGT inhibition. The finding that preSMA activation in successful stop trials was indirectly associated with inhibition efficiency in the GNGT by activation in the striatum in successful stop trials provides direct support for the cross-task context generalization of the cancel mechanism.

When defining the ROI in the rIFC, we located it in the right inferior frontal gyrus or the ventral portion of the rIFC. The contrast showed that both tasks recruited the right inferior frontal junction (rIFJ) or the ventral portion of the rIFC. This is consistent with previous findings that response inhibition recruits the rIFJ (O'Connor et al., 2015; Sebastian et al., 2016). There are two main views on the function of this region during response inhibition. Sebastian et al. (2016) argued that activation of the rIFJ is associated with attention control of salient stimulus features. This view converges with empirical evidence suggesting that

the rIFJ plays a crucial role in preparatory attentional control during feature-based attention (Meyyappan et al., 2021). In contrast, O'Connor et al. (2015) proposed that the rIFJ is responsible for representing and enforcing task rules. This view parallels the view that the IFJ plays an important role in cognitive control (Brass et al., 2005). In the present study, the activation of the rIFJ was likely to reflect the cognitive control—to guide motor response according to the task demands. However, as there were differences in visual features between the go and no-go/stop stimuli, it could not be excluded that the rIFJ reflected the attentional control of stimulus features. The experimental design of the current study did not allow us to test these two interpretations. Future studies of response inhibition should look closely at different subregions of the rIFC to delineate their functional specificity.

This study had several limitations. First, response inhibition can be further divided into reactive inhibition and proactive inhibition (Aron, 2011). Proactive inhibition refers to how people prepare to stop an upcoming response tendency. This process is goal-directed and triggered by predictive stop cues or internal signals (van Belle et al., 2014). In contrast, reactive inhibition refers to how people stop a response outright when instructed to do so by a signal (Aron, 2011). This process is stimulus-directed and triggered by salient stop signals (van Belle et al., 2014). The GNGT and the SST are two typical tasks that elicit reactive response inhibition (Aron, 2011). In the current study, we used GNGT and SST to investigate the role of rIFC and preSMA in response inhibition based on the PTC model. Therefore, it remains unknown whether the present findings and conclusions could be genderized to the proactive inhibition process. To investigate the PTC model more comprehensively, future studies should use tasks that elicit proactive inhibition (e.g., Leunissen et al., 2016 used a pre-cue to indicate the frequency of the stop stimuli; Vink et al., 2005 manipulated the expectancy of a stop trial) to re-examine the findings and conclusions of the current study.

Second, we used infrequent-go trials in the GNGT to isolate the pause process and the SST to examine the cancel process. The infrequent-go trials in the GNGT provided useful behavioral indices for testing our hypothesis regarding the pause process; however, it may have been better to examine both the pause and cancel processes in the same task. This could be achieved by using a novel experimental design, such as changing the proportion (large vs. small, e.g., 25% vs. 10%) of stop signals across blocks to manipulate the extent of stimulus salience, thereby impacting the pause process. Comparisons of the rIFC activity elicited by stop signals from different blocks may help to elucidate the neural mechanism of the pause process. In addition, the proportion of infrequent-go trials (25%) in the GNGT was higher than that in previous studies (12.3 % in Chikazoe, Jimura, Asari, et al., 2009; 12.5 % in Satoshi et al., 2012). In the Chikazoe, Jimura, Asari, et al. (2009) study, several brain regions showed an increase in signal in the “infrequent-go versus frequent-go” contrast, including the right inferior frontal area (BA 44). The relatively higher proportion (25%) of infrequent-go trials in the current study may explain why the “infrequent-go vs. frequent-go” contrast did not generate significant regions in the GNGT. Future studies using GNGT with frequent-go, infrequent-go, and no-go trials to investigate the inhibitory mechanism should include a small proportion of infrequent-go trials.

Third, we used a relatively high ratio of varied SOA for both the GNGT and the SST. Indeed, previous studies have found that including a high ratio (i.e., 50%) of jitter in the GNGT reduces cognitive control in response inhibition compared with including moderate amounts (i.e., 10%) of jitter (Wodka et al., 2009). The introduction of moderate intervals could help people to prepare for inhibition, thus facilitating inhibition control, whereas a high ratio of jitter could interfere with their ability to maintain the response set, thus resulting in poor control of inhibition (Wodka et al., 2009). According to Aron (2011), compared to tasks that can evoke preparation for a stop, tasks that trigger a stop by an external signal without preparation have limitations in examining the ability of cognitive control. However, other studies have used tasks with high jitter ratios to investigate the neural basis of the inhibition process

(Raud et al., 2020; Steele et al., 2013). Nevertheless, future studies could use a task that elicits preparation for a stop (i.e., proactive inhibition) to further examine the replication of our findings.

Fourth, due to the low temporal resolution of the fMRI technique, the current study cannot dissociate the pause and cancel processes from a temporal perspective and further capture the dynamic interactions between these two processes. Furthermore, the low temporal resolution of fMRI also brings two issues in examining the hypothesis regarding the specific role of rIFC and preSMA in response inhibition. First, we interpreted the rIFC activation in the contrast between the failed stop trials and successful go trials as an indication of the pause mechanism. However, just because a participant failed to stop does not mean there was not a cancel process triggered during the trial. In other words, a failed stop occurs when the cancel process is triggered but too slow to complete a successful stop (Diesburg and Wessel, 2021). Therefore, the greater rIFC activation in failed stop trials compared to go trials might reflect the trigger of the cancel process. Second, the significant association between preSMA activation and inhibition efficiency index supports the former's role in the cancel process. However, an alternative interpretation is that the preSMA prolonged the pause process and was not specific to a cancel process. In the current study, we tested the correlation between the preSMA activity and the pause, and the correlation between rIFC activity and inhibition efficiency indices in GNGT and SST, and found no significant results. It helps to exclude these two alternative interpretations. However, dissociating the pause and cancel processes in the temporal dimension would help to elucidate the function of rIFC and preSMA further. To achieve this, future studies should combine fMRI with high temporal resolution techniques, such as EEG and EMG, to unveil the neural basis of response inhibition from both spatial and temporal perspectives.

5. Conclusion

In this study, we employed fMRI to examine the functional specificity of rIFC and preSMA based on the PTC model. The results showed that the rIFC activation was associated with the delay of the go process, whereas the preSMA activation predicted the inhibition efficiency via striatum. This study provides direct evidence for the PTC model and insights into the neural mechanism underlying response inhibition.

Data and code availability statement

Raw data were generated from an MRI scanner. Before sharing data, the corresponding authors will make sure that all data are free of identifiers that could directly or indirectly link information to an individual and that all sharing is compliant with institutional and IRB policies.

CRediT authorship contribution statement

Lili Wu: Writing – review & editing, Writing – original draft, Formal analysis, Conceptualization. **Mengjie Jiang:** Writing – original draft, Formal analysis. **Min Zhao:** Data curation. **Xin Hu:** Data curation. **Jing Wang:** Data curation. **Kaihua Zhang:** Writing – review & editing. **Ke Jia:** Writing – review & editing. **Fuxin Ren:** Software, Formal analysis, Data curation. **Fei Gao:** Writing – review & editing, Supervision, Methodology, Funding acquisition, Conceptualization.

Declaration of competing interest

The authors declare no competing interest.

Acknowledgments

This work was supported by the National Natural Science Foundation of China (No. 81601479), Taishan Scholars Project of Shandong

Province (No. tstrup20240525), Shandong Provincial Natural Science Foundation of China (Nos. ZR2021MH030, ZR2021MH355), and Postdoctoral Innovation Projects of Shandong Province (No. SDCX-ZG-202400047).

Supplementary materials

Supplementary material associated with this article can be found, in the online version, at [doi:10.1016/j.neuroimage.2025.121004](https://doi.org/10.1016/j.neuroimage.2025.121004).

Data availability

Data will be made available on request.

References

- Aron, A.R., 2011. From reactive to proactive and selective control: developing a richer model for stopping inappropriate responses. *Biol. Psychiatry* 69 (12), e55–e68. <https://doi.org/10.1016/j.biopsych.2010.07.024>.
- Aron, A.R., Behrens, T.E., Smith, S., Frank, M.J., Poldrack, R.A., 2007. Triangulating a cognitive control network using diffusion-weighted magnetic resonance imaging (MRI) and functional MRI. *J. Neurosci.* 27 (14), 3743–3752. <https://doi.org/10.1523/jneurosci.0519-07.2007>.
- Aron, A.R., Robbins, T.W., Poldrack, R.A., 2014. Inhibition and the right inferior frontal cortex: one decade on. *Trends. Cogn. Sci.* 18 (4), 177–185. <https://doi.org/10.1016/j.tics.2013.12.003>.
- Ballanger, B., van Eimeren, T., Moro, E., Lozano, A.M., Hamani, C., Boulinguez, P., Pellecchia, G., Houle, S., Poon, Y.Y., Lang, A.E., Strafella, A.P., 2009. Stimulation of the subthalamic nucleus and impulsivity: release your horses. *Ann. Neurol.* 66 (6), 817–824. <https://doi.org/10.1002/ana.21795>.
- Brass, M., Derrfuss, J., Forstmann, B., Cramon, D.Y.v., 2005. The role of the inferior frontal junction area in cognitive control. *Trends Cogn. Sci.* 9 (7), 314–316. <https://doi.org/10.1016/j.tics.2005.05.001>.
- Brett, M., Anton, J.-L., Valabregue, R., Poline, J.-B., 2002. Region of interest analysis using the MarsBar toolbox for SPM 99. *Neuroimage* 16 (2), S497.
- Cai, W., Ryali, S., Chen, T., Li, C.S.R., Menon, V., 2014. Dissociable roles of right inferior frontal cortex and anterior insula in inhibitory control: evidence from intrinsic and task-related functional parcellation, connectivity, and response profile analyses across multiple datasets. *J. Neurosci.* 34 (44), 14652. <https://doi.org/10.1523/JNEUROSCI.3048-14.2014>.
- Cao, H., Cannon, T.D., 2021. Distinct and temporally associated neural mechanisms underlying concurrent, postsuccess, and posterror cognitive controls: evidence from a stop-signal task. *Hum. Brain Mapp.* 42 (9), 2677–2690. <https://doi.org/10.1002/hbm.25347>.
- Chikazoe, J., Jimura, K., Asari, T., Yamashita, K., Morimoto, H., Hirose, S., Miyashita, Y., Konishi, S., 2009. Functional dissociation in right inferior frontal cortex during performance of go/no-go task. *Cereb. Cortex*. 19 (1), 146–152. <https://doi.org/10.1093/cercor/bhn065>.
- Choo, Y., Matzke, D., Bowen Jr., M.D., Tranel, D., Wessel, J.R., 2022. Right inferior frontal gyrus damage is associated with impaired initiation of inhibitory control, but not its implementation. *Elife* 11. <https://doi.org/10.7554/elife.79667>.
- Corbetta, M., Shulman, G.L., 2002. Control of goal-directed and stimulus-driven attention in the brain. *Nat. Rev. Neurosci.* 3 (3), 201–215. <https://doi.org/10.1038/nrn755>.
- Corbetta, M., Patel, G., Shulman, G.L., 2008. The reorienting system of the human brain: from environment to theory of mind. *Neuron* 58 (3), 306–324. <https://doi.org/10.1016/j.neuron.2008.04.017>.
- Criaud, M., Boulinguez, P., 2013. Have we been asking the right questions when assessing response inhibition in go/no-go tasks with fMRI? A meta-analysis and critical review. *Neurosci. Biobehav. Rev.* 37 (1), 11–23. <https://doi.org/10.1016/j.neubiorev.2012.11.003>.
- Dambacher, F., Sack, A.T., Lobbestael, J., Arntz, A., Brugman, S., Schuhmann, T., 2014. A network approach to response inhibition: dissociating functional connectivity of neural components involved in action restraint and action cancellation. *Eur. J. Neurosci.* 39 (5), 821–831. <https://doi.org/10.1111/ejn.12425>.
- Diesburg, D.A., Wessel, J.R., 2021. The Pause-then-Cancel model of human action-stopping: theoretical considerations and empirical evidence. *Neurosci. Biobehav. Rev.* 129, 17–34. <https://doi.org/10.1016/j.neubiorev.2021.07.019>.
- Dutra, I.C., Waller, D.A., Wessel, J.R., 2018. Perceptual surprise improves action stopping by nonselectively suppressing motor activity via a neural mechanism for motor inhibition. *J. Neurosci.* 38 (6), 1482–1492. <https://doi.org/10.1523/jneurosci.3091-17.2017>.
- Guo, Y., Schmitz, T.W., Mur, M., Ferreira, C.S., Anderson, M.C., 2018. A supramodal role of the basal ganglia in memory and motor inhibition: meta-analytic evidence. *Neuropsychologia* 108, 117–134. <https://doi.org/10.1016/j.neuropsychologia.2017.11.033>.
- Hampshire, A., Chamberlain, S.R., Monti, M.M., Duncan, J., Owen, A.M., 2010. The role of the right inferior frontal gyrus: inhibition and attentional control. *Neuroimage* 50 (3), 1313–1319. <https://doi.org/10.1016/j.neuroimage.2009.12.109>.
- Hampshire, A., 2015. Putting the brakes on inhibitory models of frontal lobe function. *Neuroimage* 113, 340–355. <https://doi.org/10.1016/j.neuroimage.2015.03.053>.
- Hayes, A.F., 2017. *Introduction to mediation, moderation, and Conditional Process analysis: A regression-Based Approach*. Guilford publications.
- Hikosaka, O. (2007). GABAergic output of the basal ganglia. In J. M. Tepper, E. D. Abercrombie, & J. P. Bolam (Eds.), *Progress in Brain Research* (Vol. 160, pp. 209–226). Elsevier. [https://doi.org/10.1016/S0079-6123\(06\)60012-5](https://doi.org/10.1016/S0079-6123(06)60012-5).
- Hughes, M.E., Johnston, P.J., Fulham, W.R., Budd, T.W., Michie, P.T., 2013. Stop-signal task difficulty and the right inferior frontal gyrus. *Behav. Brain Res.* 256, 205–213. <https://doi.org/10.1016/j.bbr.2013.08.026>.
- Hung, Y., Gaillard, S.L., Yarmak, P., Arsalidou, M., 2018. Dissociations of cognitive inhibition, response inhibition, and emotional interference: voxelwise ALE meta-analyses of fMRI studies. *Hum. Brain Mapp.* 39 (10), 4065–4082. <https://doi.org/10.1002/hbm.24232>.
- Isherwood, S.J.S., Keuken, M.C., Bazin, P.L., Forstmann, B.U., 2021. Cortical and subcortical contributions to interference resolution and inhibition – An fMRI ALE meta-analysis. *Neurosci. Biobehav. Rev.* 129, 245–260. <https://doi.org/10.1016/j.neubiorev.2021.07.021>.
- Leunissen, I., Coxon, J.P., Swinnen, S.P., 2016. A proactive task set influences how response inhibition is implemented in the basal ganglia. *Hum. Brain Mapp.* 37 (12), 4706–4717. <https://doi.org/10.1002/hbm.23338>.
- Littman, R., Takacs, A., 2017. Do all inhibitions act alike? A study of go/nogo and stop-signal paradigms. *PLoS. One* 12 (10), e0186774. <https://doi.org/10.1371/journal.pone.0186774>. ARTN.
- Logan, G.D., Cowan, W.B., 1984. On the ability to inhibit thought and action: a theory of an act of control. *Psychol. Rev.* 91 (3), 295–327. <https://doi.org/10.1037/0033-295X.91.3.295>.
- Maizley, L., Evans, C.J., Muhlert, N., Verbruggen, F., Chambers, C.D., Allen, C.P.G., 2020. Cortical and subcortical functional specificity associated with response inhibition. *Neuroimage* 220, 117110. <https://doi.org/10.1016/j.neuroimage.2020.117110>.
- Mcnab, F., Leroux, G., Strand, F., Thorell, L., Bergman, S., Klingberg, T., 2008. Common and unique components of inhibition and working memory: an fMRI, within-subjects investigation. *Neuropsychologia* 46 (11), 2668–2682. <https://doi.org/10.1016/j.neuropsychologia.2008.04.023>.
- Meyyappan, S., Rajan, A., Mangun, G.R., Ding, M., 2021. Role of Inferior Frontal Junction (IFJ) in the Control of Feature versus Spatial Attention. *J. Neurosci.* 41 (38), 8065–8074. <https://doi.org/10.1523/jneurosci.2883-20.2021>.
- Mostofsky, S.H., Schafer, J.G.B., Abrams, M.T., Goldberg, M.C., Flower, A.A., Boyce, A., Courtney, S.M., Calhoun, V.D., Kraut, M.A., Denckla, M.B., Pekar, J.J., 2003. fMRI evidence that the neural basis of response inhibition is task-dependent. *Cogn. Brain Res.* 17 (2), 419–430. [https://doi.org/10.1016/S0926-6410\(03\)00144-7](https://doi.org/10.1016/S0926-6410(03)00144-7).
- Nakata, H., Sakamoto, K., Ferretti, A., Gianni Perrucci, M., Del Gratta, C., Kakigi, R., Luca Romani, G., 2008. Somato-motor inhibitory processing in humans: an event-related functional MRI study. *Neuroimage* 39 (4), 1858–1866. <https://doi.org/10.1016/j.neuroimage.2007.10.041>.
- O'Connor, D.A., Upton, D.J., Moore, J., Hester, R., 2015. Motivationally significant self-control: enhanced action withholding involves the right inferior frontal junction. *J. Cogn. Neurosci.* 27 (1), 112–123. https://doi.org/10.1162/jocn_a_00695.
- Quetscher, C., Yıldız, A., Dharmadhikari, S., Glaubitz, B., Schmidt-Wilcke, T., Dydak, U., Beste, C., 2015. Striatal GABA-MRS predicts response inhibition performance and its cortical electrophysiological correlates. *Brain Struct. Funct.* 220 (6), 3555–3564. <https://doi.org/10.1002/s00429-014-0873-y>.
- Rae, C.L., Hughes, L.E., Anderson, M.C., Rowe, J.B., 2015. The prefrontal cortex achieves inhibitory control by facilitating subcortical motor pathway connectivity. *J. Neurosci.* 35 (2), 786–794. <https://doi.org/10.1523/JNEUROSCI.3093-13.2015>.
- Raud, L., Westerhausen, R., Dooley, N., Huster, R.J., 2020. Differences in unity: the go/no-go and stop signal tasks rely on different mechanisms. *Neuroimage* 210, 116582. <https://doi.org/10.1016/j.neuroimage.2020.116582>.
- Reisenzein, R., Meyer, W.U., Niepel, M., 2012. Surprise. In: Ramachandran, V.S. (Ed.), *Encyclopedia of Human Behavior*, 2nd Edition. Academic Press, pp. 564–570. <https://doi.org/10.1016/B978-0-12-375000-6.00353-0>.
- Satoshi, H., Junichi, C., Takamitsu, W., Koji, J., Akira, K., Osamu, A., Kuni, O., Yasushi, M., Seiki, K., 2012. Efficiency of go/no-go task performance implemented in the left hemispheric. *J. Neurosci.* 32 (26), 9059. <https://doi.org/10.1523/JNEUROSCI.0540-12.2012>.
- Schaum, M., Pinzuti, E., Sebastian, A., Lieb, K., Fries, P., Mobsacher, A., Jung, P., Wibral, M., Tüscher, O., 2021. Right inferior frontal gyrus implements motor inhibitory control via beta-band oscillations in humans. *Elife* 10. <https://doi.org/10.7554/elife.61679>.
- Schevernels, H., Bombeke, K., Van der Borght, L., Hopf, J.-M., Krebs, R.M., Boehler, C.N., 2015. Electrophysiological evidence for the involvement of proactive and reactive control in a rewarded stop-signal task. *Neuroimage* 121, 115–125. <https://doi.org/10.1016/j.neuroimage.2015.07.023>.
- Schmidt, R., Berke, J.D., 2017. A Pause-then-Cancel model of stopping: evidence from basal ganglia neurophysiology. *Philos. Trans. R. Soc. B Biol. Sci.* 372 (1718), 20160202. <https://doi.org/10.1098/rstb.2016.0202>.
- Sebastian, A., Konken, A.M., Schaum, M., Lieb, K., Tüscher, O., Jung, P., 2021. Surprise: unexpected action execution and unexpected inhibition recruit the same fronto-basal-ganglia network. *J. Neurosci.* 41 (11), 2447–2456. <https://doi.org/10.1523/jneurosci.1681-20.2020>.
- Simmonds, D.J., Pekar, J.J., Mostofsky, S.H., 2008. Meta-analysis of Go/No-go tasks demonstrating that fMRI activation associated with response inhibition is task-dependent. *Neuropsychologia* 46 (1), 224–232. <https://doi.org/10.1016/j.neuropsychologia.2007.07.015>.
- Steele, V.R., Aharoni, E., Munro, G.E., Calhoun, V.D., Nyakalanti, P., Stevens, M.C., Pearson, G., Kiehl, K.A., 2013. A large scale (N=102) functional neuroimaging study of response inhibition in a Go/NoGo task. *Behav. Brain Res.* 256, 529–536. <https://doi.org/10.1016/j.bbr.2013.06.001>.

- Swick, D., Ashley, V., Turken, U., 2011. Are the neural correlates of stopping and not going identical? Quantitative meta-analysis of two response inhibition tasks. *Neuroimage* 56 (3), 1655–1665. <https://doi.org/10.1016/j.neuroimage.2011.02.070>.
- Tatz, J.R., Soh, C., Wessel, J.R., 2021. Common and unique inhibitory control signatures of action-stopping and attentional capture suggest that actions are stopped in two stages. *J. Neurosci.* 41 (42), 8826–8838. <https://doi.org/10.1523/jneurosci.1105-21.2021>.
- van Belle, J., Vink, M., Durston, S., Zandbelt, B.B., 2014. Common and unique neural networks for proactive and reactive response inhibition revealed by independent component analysis of functional MRI data. *Neuroimage* 103, 65–74. <https://doi.org/10.1016/j.neuroimage.2014.09.014>.
- Verbruggen, F., Logan, G.D., 2008. Response inhibition in the stop-signal paradigm. *Trends Cogn. Sci.* 12 (11), 418–424. <https://doi.org/10.1016/j.tics.2008.07.005>.
- Vink, M., Kahn, R.S., Raemaekers, M., van den Heuvel, M., Boersma, M., Ramsey, N.F., 2005. Function of striatum beyond inhibition and execution of motor responses. *Hum. Brain Mapp.* 25 (3), 336–344. <https://doi.org/10.1002/hbm.20111>.
- Wadsley, C.G., Cirillo, J., Nieuwenhuys, A., Byblow, W.D., 2023. A global pause generates nonselective response inhibition during selective stopping. *Cereb. Cortex* 33 (17), 9729–9740. <https://doi.org/10.1093/cercor/bhad239>.
- Weber, S., Salomoni, S.E., Kilpatrick, C., Hinder, M.R., 2023. Dissociating attentional capture from action cancellation during the inhibition of bimanual movement. *Psychophysiology* 60 (11), e14372. <https://doi.org/10.1111/psyp.14372>.
- Wessel, J.R., Aron, A.R., 2015. It's not too late: the onset of the frontocentral P3 indexes successful response inhibition in the stop-signal paradigm. *Psychophysiology* 52 (4), 472–480. <https://doi.org/10.1111/psyp.12374>.
- Wessel, J.R., Aron, A.R., 2017. On the globality of motor suppression: unexpected events and their influence on behavior and cognition. *Neuron* 93 (2), 259–280. <https://doi.org/10.1016/j.neuron.2016.12.013>.
- Wodka, E.L., Simmonds, D.J., Mahone, E.M., Mostofsky, S.H., 2009. Moderate variability in stimulus presentation improves motor response control. *J. Clin. Exp. Neuropsychol.* 31 (4), 483–488. <https://doi.org/10.1080/13803390802272036>.
- Xu, B., Sandrini, M., Wang, W.T., Smith, J.F., Sarlls, J.E., Awosika, O., Butman, J.A., Horwitz, B., Cohen, L.G., 2016. PreSMA stimulation changes task-free functional connectivity in the fronto-basal-ganglia that correlates with response inhibition efficiency. *Hum. Brain Mapp.* 37 (9), 3236–3249. <https://doi.org/10.1002/hbm.23236>.
- Zheng, D., Oka, T., Bokura, H., Yamaguchi, S., 2008. The key locus of common response inhibition network for no-go and stop signals. *J. Cogn. Neurosci.* 20 (8), 1434–1442. <https://doi.org/10.1162/jocn.2008.20100>.